AFRL-OSR-VA-TR-2013-0012

Transition Metal Complex/Polymer Systems as Optical Limiting Materals

Russell Schmehl, Igor Rubtsov
Tulane University

May 2013
Final Report

AIR FORCE RESEARCH LABORATORY
AF OFFICE OF SCIENTIFIC RESEARCH (AFOSR)
ARLINGTON, VIRGINIA 22203
AIR FORCE MATERIEL COMMAND

REPORT DOCUMENTATION PAGE

Form Approved
OMB No. 0704-0188

PLEASE DO NOT RETURN YOUR FORM TO THE ABOVE ORGANIZATION.

1. REPORT DATE *(DD-MM-YYYY)*	2. REPORT TYPE	3. DATES COVERED *(From - To)*
13-01-2013	Final	Oct. 2009 - Dec. 2013

4. TITLE AND SUBTITLE
Transition Metal Complex/ Polymer Systems as Optical Limiting Materials

5a. CONTRACT NUMBER

5b. GRANT NUMBER
FA9550-10-1-0007

5c. PROGRAM ELEMENT NUMBER

6. AUTHOR(S)
Schmehl, Russell H.
Rubtsov, Igor V.

5d. PROJECT NUMBER

5e. TASK NUMBER

5f. WORK UNIT NUMBER

7. PERFORMING ORGANIZATION NAME(S) AND ADDRESS(ES)
Tulane University
Department of Chemistry
New Orleans, LA 70118

8. PERFORMING ORGANIZATION REPORT NUMBER

9. SPONSORING/MONITORING AGENCY NAME(S) AND ADDRESS(ES)
AFOSR/RSA
875 North Randolph Street
Suite 325, Room 3112
Arlington, VA 22203

10. SPONSOR/MONITOR'S ACRONYM(S)
AFOSR/RSA

11. SPONSOR/MONITOR'S REPORT NUMBER(S)
AFRL-OSR-VA-TR-2013-0012

12. DISTRIBUTION/AVAILABILITY STATEMENT
A-Unlimited Distribution A: Approved for public release

13. SUPPLEMENTARY NOTES
None

14. ABSTRACT
This project was directed toward the generation of long wavelength visible optical limiting materials that respond via a combination of reverse saturable absorption and two-photon absorption processes. The particular wavelength range we have focused on initially is the 600-900 nm range, covering frequencies of regeneratively amplified Ti:sapphire lasers. The chromophores all have two relatively independent chromophoric systems as a part of their structure. One system is optimized to exhibit one or two photon absorption in the long wavelength visible region and the other, accessed by population of the first, allows optimization of the transient absorption of light that will provide the optical limiting effect. This report discusses our work in three areas: (a) the design and synthesis of ligands and metal complex systems that approach optimization of the two chromophoric components, (b) photophysical characterization and evaluation of the figures of merit for the chromophores and (c) evaluation of the dissipation of vibrational excitation energy of model chromophores using relaxation assisted two-dimensional infrared spectroscopy.

15. SUBJECT TERMS
Optical Limiting, Reverse Saturable Absorption, Two-photon Absorption, Transition metal complex photochemistry, Time resolved vibrational spectroscopy, 2DIR, Infrared photon echo

16. SECURITY CLASSIFICATION OF:			17. LIMITATION OF ABSTRACT	18. NUMBER OF PAGES	19a. NAME OF RESPONSIBLE PERSON
a. REPORT	b. ABSTRACT	c. THIS PAGE			Russell Schmehl
U	U	U	SAR		19b. TELEPHONE NUMBER *(Include area code)* 504-862-3566

Introduction

This project was directed toward the generation of long wavelength visible optical limiting materials that respond via a combination of reverse saturable absorption and two-photon absorption processes. The particular wavelength range we have focused on initially is the 600-900 nm range, covering frequencies of regeneratively amplified Ti:sapphire lasers. The chromophores all have two relatively independent chromophoric systems as a part of their structure. One system is optimized to exhibit one or two photon absorption in the long wavelength visible region and the other, accessed by population of the first, allows optimization of the transient absorption of light that will provide the optical limiting effect. This report discusses our work in three areas: (a) the design and synthesis of ligands and metal complex systems that approach optimization of the two chromophoric components, (b) photophysical characterization and evaluation of the figures of merit for the chromophores and (c) the study of vibrational energy dissipation in model systems excited in the infrared and involving relaxation assisted two-dimensional infrared spectroscopy.

The chromophores prepared all contain transition metal complexes of Ru(II) or Os(II) with ligands tailored to coordinate to the metal center and include a separate light absorbing center with strong excited state absorption in the wavelength region of interest. A state diagram for such a complex is shown in Fig. 1. In the majority of M(II) diimine complexes, the ground and excited state absorption is dominated by the metal-to-ligand charge transfer (MLCT) transitions. Upon covalent linkage of an aromatic hydrocarbon having a localized triplet state (^{3}IL) of energy comparable to, but slightly lower than, the ^{3}MLCT, excitation energy can migrate from the ^{3}MLCT state to the ^{3}IL state. The intersystem crossing to populate the triplet and the internal conversion to generate the ^{3}IL state should occur on the 1-100 ps time scale. With the right choice of aromatic hydrocarbon, there can be unique advantages that dramatically alter the optical limiting behavior of the complex. Exploration of the magnitude of the associated optical limiting is the focus of the work. In the sections below, the phases of the work are discussed.

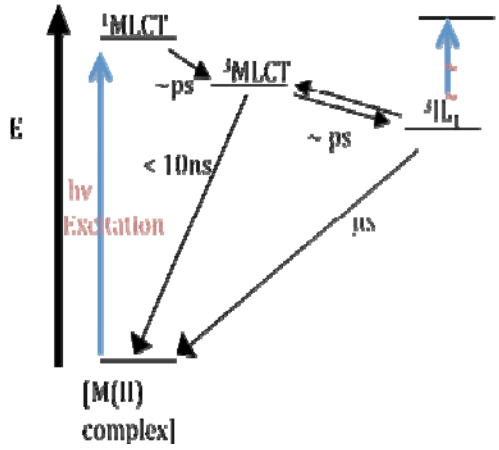

Figure A1 : State diagram for complexes.

A. Synthesis and Spectroscopy of ligands and complexes:

1. Synthesis: The concept for ligand synthesis was to have aromatic hydrocarbon containing ligands with vinyl substituents linking the aromatic portion of the molecule and the coordinating ligand. The vinyl (rather than perhaps acetylide) is important because it impacts the energy of the ^{3}IL state in a significant way, lowering it so that the energy of the absorbing metal complex chromophores can also be lowered into the long wavelength region of the visible. The inclusion of a vinyl substituents lowers the energy of the triplet ligand localized state by as much as 2000 cm^{-1} . The synthetic strategy, presented as a retrosynthesis, is shown below in Fig. A2. The coupling of the aldehyde with the bipyridyl or terpyridyl reagent is via a Wittig or Horner –

Wadsworth-Emmons (HWE) intermediate phosphorous compound. Fig. A2 illustrates specifically the HWE approach for a series of bipyridyl derivatives. The approach uses commercially available 4,4'-dimethyl-2,2'-bipyridine which is converted to the phosphonate by reaction of the intermediate bromide with triethylphosphite. The intermediate phosphonate is stable and can be stockpiled. The subsequent HWE coupling with an aromatic aldehyde makes use of commercially available aldehydes for all the ligands except the perylene. Thus, for most of the derivatives, the products can be obtained in three straightforward steps to yield the desired ligands. The reaction sequence can also be carried out with a commercially available terpyridyl derivative that goes through the same types of intermediates. Properties of complexes made with both sets of ligands will be presented below.

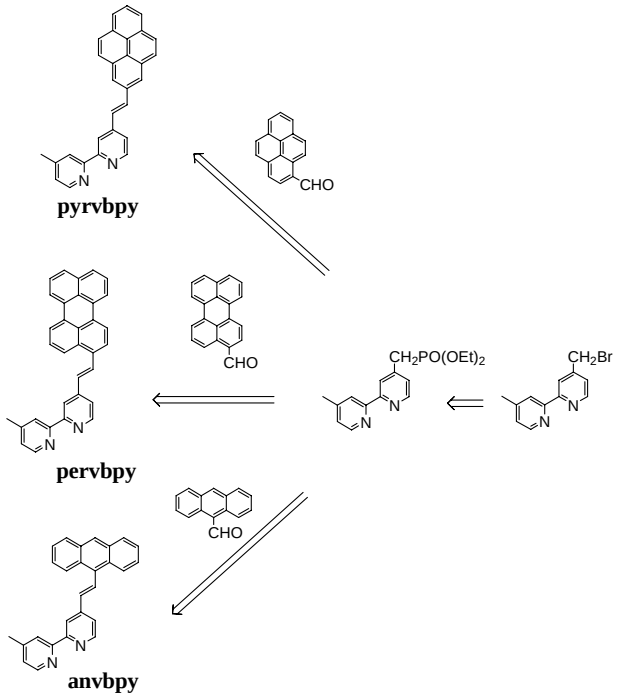

It is possible that the torsional flexibility of this class of ligands, with possible trans-cis isomerization of the vinyl group, could contribute to a very high density of states that lead to relaxation to the ground state rather than formation of the thermally equilibrated intraligand triplet excited state.

Figure A2: Retrosynthesis of ligands for RSA development.

An approach to dealing with this is to make other ligands that have a higher degree of structural rigidity, thereby removing many low frequency modes for nonradiative relaxation from the singlet excited state. Our general approach to making such ligands is shown below for the ligand BDPZ. Two other ligands prepared with similar methodology are also shown below.

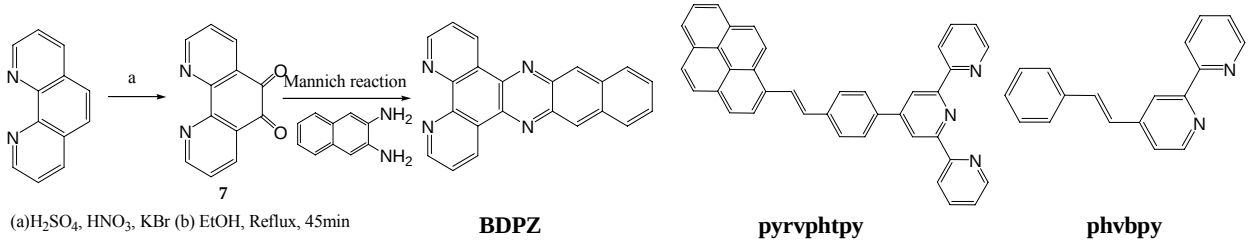

A wide range of metal complexes can be synthesized using the ligand set generated. The objective for the bipyridyl ligands is to make complexes with one or two of the aromatic hydrocarbon modified bipyridines and control the visible light absorption characteristics with the remaining two coordination sites. Figure A3 shows a complex having two pyrene-vinyl-bipyridyl (*pyrvbpy*) ligands and two chloride ligands. The optical properties of the chromophores can be tuned by substituting the chloride ligands with ligands such as ammonia, ethylene diamine, thiolates, thiocyanate, cyanide, etc. In addition, tris-heteroleptic complexes can be made which

have only a single *pyrvbpy* (or other bipyridyl) ligand and another bidentate ligand (such as bipyridine, phenanthroline or substituted bipyridines). The visible light absorption of the metal center is controlled by variation of the metal of the complex and the nature of the spectator ligands. The spectral range over which the uv-vis absorption can be tuned by substitution on Ru(II) centers alone is greater than 100 nm (between approximately 450 nm and 600 nm). Following absorption of visible light (or two photon excitation) the excitation energy migrates to the pyrene vinyl bipyridyl ligand which provides the chromophores that gives rise to the excited state absorption.

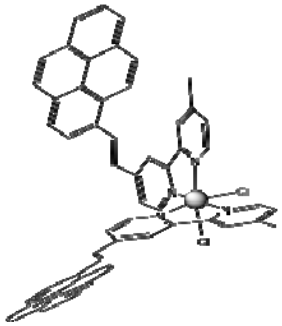

Figure A3 : Representation of $[M(pyrvbpy)_2Cl_2]$

A separate issue involves the deep colors of the Ru(II) complexes we have prepared to date. While the complexes *are* transparent in the 600 – 900 nm range, they have deep red / red-orange colors and complexes of greater transparency in the visible would clearly be preferred. Our approach will be to make Re(I) and Pt(II) complexes with the ligands already prepared including pyrvbpy and pyrvphtpy; we are just now (end of third year of project) beginning photophysical measurements of various Re(I) complexes. The Re(I) complexes have an additional coordination site to tune the excited state energy and provide for a long lived excited state lifetime; these complexes typically have allowed absorption further to the blue. For instance, reaction of $[Re(CO)_5Cl]$ with pyr-v-bpy yields $[(pyr\text{-}v\text{-}bpy)Re(CO)_3Cl]$; further reaction with π accepting ligands such as pyridine or acetonitrile will yield complexes that, by comparison with complexes in the literature, will have long excited state lifetimes and have excited state absorption in the red portion of the visible. The key additional requirement is a large two-photon absorption coefficient at wavelengths where excited state absorption is strongest or some degree of linear absorption in the red (very likely resulting from spin-forbidden Re to pyr-v-bpy MLCT absorption).

A final aspect of the ligand and complex design not addressed at present is the materials compatibility of the complexes for incorporation into polymer films. This can be controlled by synthetic modification of a bipyridyl ligand and by control of the charge of the complex. Results of this work are discussed in section D.

2. Photophysical characterization and evaluation of the figures of merit for the chromophores: The complexes prepared were all evaluated by absorption, luminescence and transient absorption spectroscopy in order to determine the excited state to ground state absorption cross section ratio. The ratio is a critical figure of merit in evaluating potential optical limiters based on reverse saturable absorption.

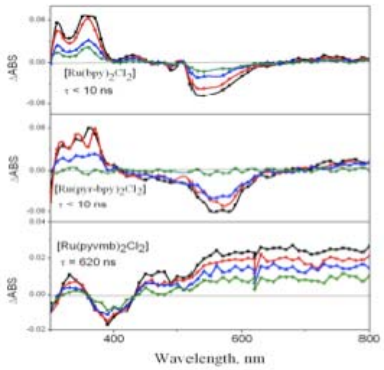

Figure A4: Transient absorption spectra of Ru(II) complexes in acetonitrile

A key characteristic of the dual chromophore systems prepared is that the aromatic hydrocarbon component associated with the complex serves to extend the excited state lifetime and gives rise to the long wavelength excited state absorption important to optical limiting. This is nicely illustrated by comparing the transient absorption spectra of the complex $[(pyrvbpy)_2RuCl_2]$, $[(pyrbpy)_2RuCl_2]$ (pyrbpy = 4-pyrenyl-2,2'-bipyridine) and $[(bpy)_2RuCl_2]$ (bpy = 2,2'-bipyridine). Figure A4 shows both ground state absorption and transient absorption for the three; the excited state of the bpy complex has a lifetime of less than 10 ns, while that of the

Table I . Complex	λ_{max} , nm	λ_{max} , nm Trans Abs	τ_{TA}, ns	$\varepsilon_{ex.\ st}$, $M^{-1}\ cm^{-1}$	$\varepsilon_{eex\ st}/\varepsilon_{gr\ st}$ 650 nm	$\varepsilon_{eex\ st}/\varepsilon_{gr\ st}$ 750 nm
$[(pyrvbpy)Ru(bpy)_2]^{2+}$	460	600, 750(sh)	5000	40,000	60	150
$[(pyrvbpy)_2Ru(en)]$	410, 550	700	700	28,000	40	125
$[(pyrvbpy)_2RuCl_2]^{2+}$	390, 590	700	620	20,000	10	25
$[(pyrvphtpy)Ru(dien)]^{2+}$	390, 550	750	600	> 20000	--	--
$[(pyrvphtpy)_2Ru]^{2+}$	380, 500	720	9000	> 20000	--	--
$[(pyrvphtpy)Ru(CN)_3]^{-1}$	390, 500	750	7000	>20,000	--	--
$[(bpy)_2Ru(BDPZ)]^{2+}$	302, 428	550	50000	---	---	---
$[(bpy)_2Ru(phvbpy)]^{2+}$	284, 458		130			
$[(pyrvphtpy)_2Os]^{2+}$	500, 650	590, 740	1400	--	--	--

pyrvbpy complex has a lifetime of 620 ns in acetonitrile. An important additional point is that the complex with a pyrene ligand lacking the additional vinyl behaves nearly the same as the *unsubstituted* bpy complex. It is only the pyrvbpy complex (and complexes of related ligands) that exhibits the long wavelength transient absorption and extended excited state lifetime. This is because only in the pyrvbpy complex is the ^{3}IL state lower in energy than the ^{3}MLCT state.

A part of the excited state absorption measurement involves determination of the absorptivity of the excited state. Our approach to this measurement was to use the energy transfer method. This is accomplished by quenching the metal complex excited state, formed by direct excitation, with a molecule that does not competitively absorb excitation light, that quenches the metal complex excited state and that has a known excited state absorption coefficient. For the complexes discussed in this report, the triplet excited state energies are very low (< 14,000 cm^{-1}) and tetracene is one of a small number of potential quenchers that meet the requirements above. The absorbance of the energy acceptor (tetracene) is measured for the complex following quenching of the excited metal complex and the absorptivity of the metal complex excited state is then determined using the expression below where ΔA corresponds to the measured transient absorbance signal immediately after excitation for the metal complex alone and immediately following energy transfer quenching for the energy acceptor, ε represents the excited state molar absorptivity and *f* is the fraction of metal complex excited states quenched by the energy acceptor. The absorptivity of the complex is described as a difference in absorptivity between the ground and excited states because that is what is measured.

$$\Delta\varepsilon_{complex} = \varepsilon_{acceptor}(\Delta A_{complex}/\ \Delta A_{acceptor})\ f$$

In most of the complexes the ground state absorptivity is very small at longer wavelengths where the transient absorbance is strongest and is subtracted after determination of $\Delta\varepsilon$. Table I includes data accumulated for the complexes prepared thus far; excited state absorptivities have only been determined for a few of the complexes and the additional ratios of excited state to ground

state cross sections at 650 and 750 nm do not reveal the optimal spectral windows for the complexes. All of the complexes with the pyrv component exhibit strong excited state absorbance in the 650 – 800 nm region and the cross section ratio (and potential utility) is influenced most strongly by the ground state absorbance in this spectral region. The capability of the complexes to function as reverse saturable absorbers requires some long wavelength absorption. In this regard the Os(II) complex of Table I seems most promising as it has a spin forbidden MLCT absorption that extends to 700 nm as well as the excited state absorption imparted by the pyrv moiety. The promise exists that some of these chromophores will have large ratios of excited state to ground state cross section over bands of wavelength in the 600-800 nm region *and* will have excited state lifetimes of at least 1 microsecond.

Earlier it was mentioned that the BDPZ ligand was prepared as a means of decreasing the nonradiative relaxation rate of the complexes through rigidification of the ligand. Table I indicates that the strategy worked for increasing the excited state lifetime, but, as shown in figure A5, the excited state absorption has a maximum of approximately 550 nm and only weak absorption farther to the red. The need for the pyrene substituent on the ligand is illustrated

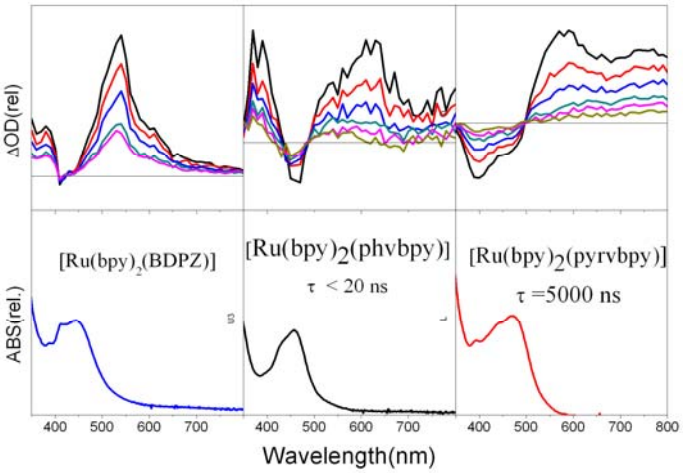

Figure A5 . Transient spectra of potential reverse saturable absorbers

by comparison of the phvbpy and the pyrvbpy complexes. The spectra of the two complexes are similar, but the signal size is larger and excited state lifetime is orders of magnitude longer for the pyrvbpy complex.

Another characteristic of effective optical limiting is the efficiency with which the initially formed singlet excited state forms the long lived triplet state with the strong excited state absorbing component. We employed the above energy transfer quenching approach to determine the yield of singlet excited states formed that produce the pyrv containing triplet. Looking at figure A1, it is clear that the first state formed is the singlet MLCT state and that this state very likely passes through the triplet MLCT state en route to forming the pyrv localized triplet. The intermediate triplet MLCT state may have relaxation channels that compete with crossover to the triplet IL state (excited pyrv in most of the complexes). Results for intersystem crossing yields are given in Table 2 for some of the complexes studied. The parent complex $[Ru(bpy)_3]^{2+}$ is known to have an intersystem crossing yield of unity and is included to illustrate the margin of error in the measurement. While there remains some question regarding the

Table 2. Complex	TA λ_{max} , nm	η_{isc}
$[Ru(bpy)_3]^{2+}$	460	0.89 ± 0.1
$[Ru(bp\text{-}vpyr)_2Cl_2]$	700	0.07 ± 0.02
$[Ru(bp\text{-}vpyr)_2(en)]^{2+}$	700	0.22 ± 0.02
$[Ru(bp\text{-}vpyr)(bpy)_2]^{2+}$	600, 750 (sh)	0.40 ± 0.05
$[Ru(bpy)_2(BDPZ)]^{2+}$	700	0.50 ± 0.02

accuracy of the values obtained, the implication is that, for some of the complexes, a significant fraction of the excited states formed may never reach the strongly absorbing triplet IL (pyrv localized) state. The implication of this is that the measured excited state absorbance will be lower than theoretically possible following absorption of a photon and this would have a direct effect on the effectiveness of a given reverse saturable absorber. It is commonly believed to be the case that, for nearly all Ru(II) diimine complexes, the intersystem crossing efficiency to populate the triplet state is close to unity. We are continuing to pursue other means of determining these intersystem crossing efficiencies to evaluate the validity of these figures.

B. Determination of two-photon absorption cross-sections

B.1. Schematics and performance of the z-scan apparatus

The z-scan apparatus has been designed and implemented at Tulane in October 2010 (Fig. B1). It uses a Ti:Sapphire laser at 800 nm with 1 kHz repetition rate and ca. 80 fs pulse duration. To ensure reliable operation we performed extensive testing of the setup. We found that it is essential to reduce the repetition rate of the laser (800 nm, 1 kHz, pulse duration ~80 ps) from 1 kHz to 50 Hz. This allowed eliminating the thermal lens contribution to the signal, which perturbed substantially the measured z-scan traces in both opened- and closed- aperture measurements thus limiting severely the setup sensitivity. Repetition rate reduction permitted complete elimination of the thermal contribution (the thermal contribution dropped below the

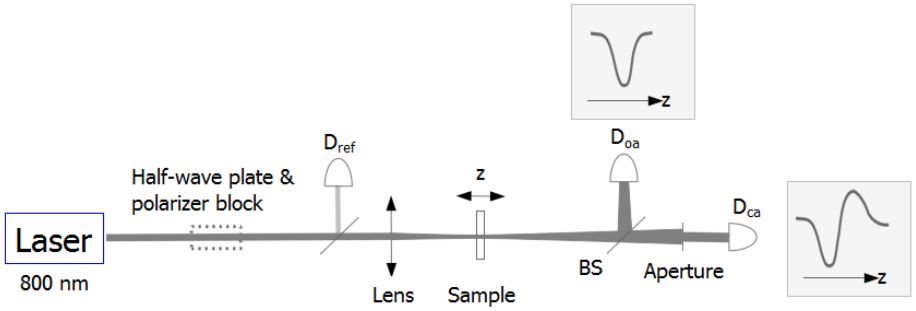

Fig. B1. Z-scan setup schematics. Here D_{oa}, D_{ca}, and D_{ref} are the opened-aperture, closed-aperture, and reference detectors, respectively, BS is the beam splitter, the focal length of the lens is 400 mm.

noise level). A sensitivity of ca. 0.05% was achieved in the opened-aperture measurements with averaging of just 10 laser shots per point (Fig. B2). The linearity of the z-scan amplitude (transmission reduction) as a function of concentration has been confirmed (Fig. B3A). Then linearity of the z-scan amplitude to the laser intensity has been tested (Fig. B3B) and the range of powers suitable for measurements has been determined (< 0.4 μJ/pulse). Note that the linearity of the detectors essential in these measurements was controlled accurately. Two test samples with known two-photon absorption cross sections were selected. One was a 2 mm thick ZnSe wafer, another was the O1 (Fig. B3) compound synthesized in the Schmehl laboratory. The two-photon absorption cross-section obtained for the ZnSe wafer (3.1 cm/GW) was found to be within 20% from the reported value (3.87 cm/GW). The two-photon cross-section for O1 was measured at 1300 GM, which differed substantially from the reported values of 381 GM; since the TPA cross-section of ZnSe is more reliable, the ZnSe wafer was routinely used as a reference

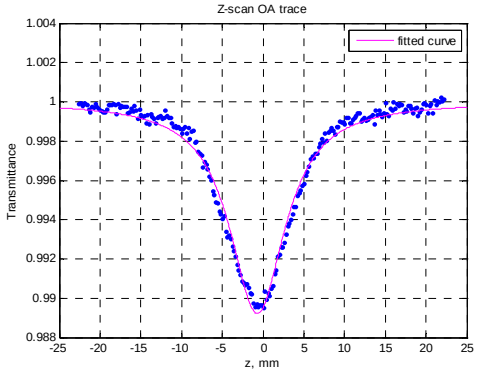

Fig. B2. (A) Opened-aperture z-scan trace for [Ru(pyrvph-tpy)$_2$][PF$_6$]$_2$ measured with 10 laser short accumulations per point at 3 μJ per pulse energy and 10 Hz laser repetition rate.

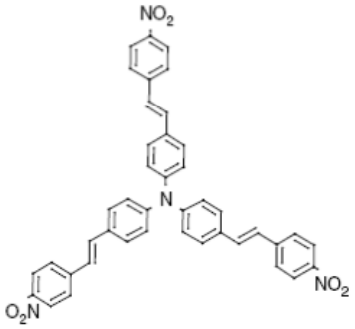

Fig. B3. Octupolar molecule O1. (G.J. Lee et al., Current Applied Physics 4 (2004) 573).

sample. The laser beam diameter in the focus and off the focus were carefully measured (Fig. B4C).

Z-scan measurements at 800 nm were performed for several Ru and Os complexes (Table 1). Several compounds were found to show very respectable two-photon absorption cross

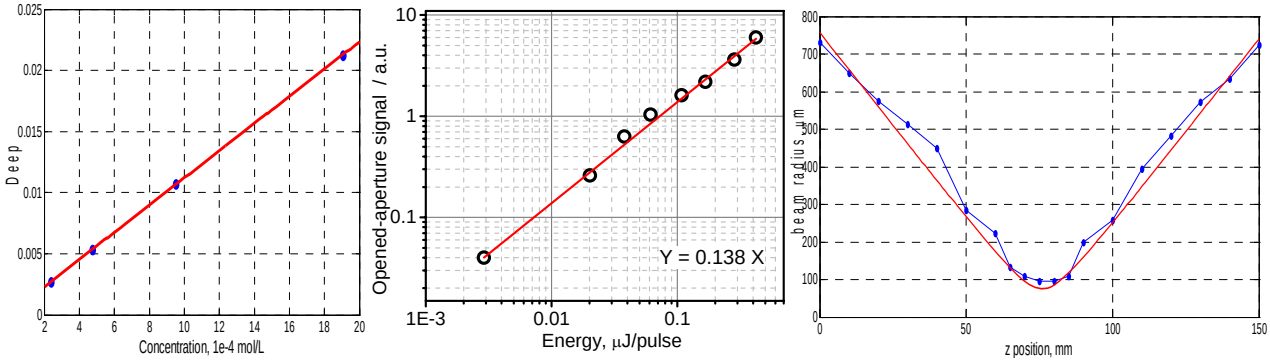

Fig. B4. (A) Dependence of the z-scan amplitude (deep) at the minimum as a function of the sample concentration (0.3 μJ/pulse laser power). (B) Z-scan amplitude at the focus as a function of laser power. Both dependencies were measured for the [Ru(pyr-v-ph-bpy)$_2$(en)](PF$_6$)$_2$ complex. (C) Laser beam profile.

sections, including the Ruthenium complex featuring two pyrenyl-vinyl-phenyl-bipyridine ligands which demonstrated exceptional σ of 3700 GM at 800 nm.

Table 1. Two-photon absorption cross sections measured for a set of Ru and Os compounds at 800 nm wavelength using a z-scan method. Extinction coefficients for the compounds at 800 nm are also shown.

Compounds	ε at 800 nm / $M^{-1}cm^{-1}$	σ at 800 nm / GM
[Ru(pyrvphtpy)$_2$][PF$_6$]$_2$	28.9	470
[Ru(pyrvphtpy)(dien)][PF$_6$]$_2$	182	990
[Os(pyrvphtpy)$_2$][PF$_6$]$_2$	2443	1330
[Ru(pyrvphbpy)$_2$(en)](PF$_6$)$_2$	< 10	3700
[Ru(pyrbpy)(bpy)$_2$](Cl)$_2$	< 10	440
[Ru(pyrphbpy)(bpy)$_2$](PF$_6$)$_2$	< 10	400

Ligand notation: (pyr-) – pyrenyl, (v-) – vinyl, (ph-) – phenyl, (bpy) – bipyridine, (tpy) – terpyridine, (dien) – diethylenetriamine, (en) – ethylenediamine.

C. Ultrafast visible pump-probe experiments

The scheme for generating excited states that absorb well in the 600-800 nm range depends strongly on an intramolecular energy transfer process between the initially populated charge transfer state via either direct or two-photon excitation and an excited state localized on one of the coordinated ligands. The figure below shows the state diagram for these materials. Of concern is the rate at which the initially excited ^{1}MLCT state evolves to form the ^{3}IL state that serves as the strong excited state absorber in the near-infrared. To approach this question, we developed a collaboration with the group of Tim Liam at Emory University. Using a pump-probe experiment involving < 100 femtosecond excitation and probing of the difference absorption spectrum in the visible in the fs to ns time regime, we were able to elucidate the dynamics of the intramolecular energy migration following direct excitation of the ^{1}MLCT state. Figures C1 and C2 illustrates the changes observed for $[(pyrvphtpy)_2Ru]^{2+}$ in acetonitrile solution on the nanosecond and on the femtosecond time scales. The significant observation from this comparison is that the

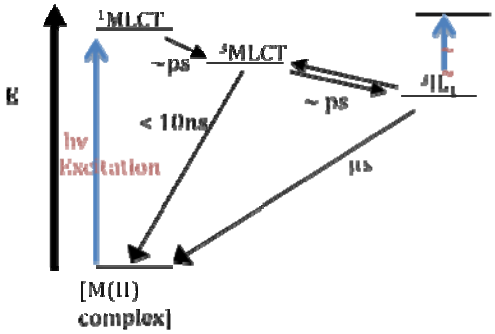

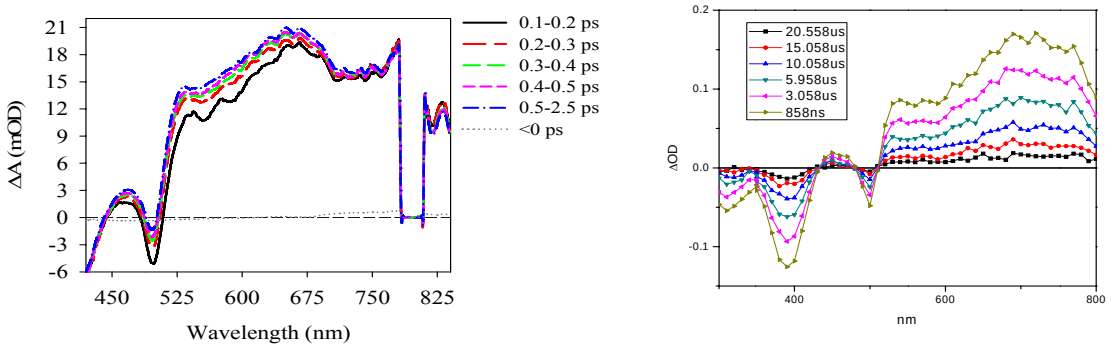

C. 1 Absorption changes in the first 2.5 ps following excitation of $[(pyrvphtpy)_2Ru]^{2+}$ in CH_3CN (left) and C.2 Nanosecond transient absorption spectra.

absorbing transient in the red portion of the spectrum is formed essentially instantaneously following excitation. This is an important point because the excited state responsible for the optical limiting phenomenon is a triplet excited state that differs from the initially formed singlet MLCT state. Comparison with other complexes having a pyrene and bipyridine linked to a Ru(II) center indicates that the associated vinyl group has a significant accelerating effect on the rate of formation of the long wavelength absorbing transient. The same sub-ps timescale for formation of the long wavelength absorbing transient has been observed for $[(pyrvbpy)_2Ru(en)]^{2+}$ (en = ethylenediamine) and $[(pyrvphtpy)Ru(dien)]^{2+}$. A manuscript is in preparation on this work. Additional work with chromophores having a range of ligands with substituents that absorb in the near-infrared is planned; the emphasis will be on determination of the rate constant for internal conversion from the ^{3}MLCT state to the ^{3}IL state.

D. Cast films of complexes in PMMA, PVA or other polymer matrices

Ultimately the chromophores developed must be incorporated into a solid state matrix in order to be of practical use. Since the complexes prepared for this purpose are salts, the issue of dissolving them in a polymer matrix is significant. Fortunately, these complexes contain hydrophobic ligands and are readily soluble in a wide variety of organic solvents. In addition, the desired optical behavior is an intramolecular phenomenon and diffusion in the polymer matrix is not a requirement. In the past we have had significant success incorporating Ru(II) complexes in polymethyl methacrylate (PMMA) matrices. Now that we have identified several promising chromophores, we are beginning these experiments. The polymers are prepared by heating (3hr) a degassed solution of the monomer containing dissolved chromophore and including a small amount of a radical initiator. Initial work with $[Ru(pyr\text{-}v\text{-}bpy)_2(en)](PF_6)_2$ incorporated into PMMA matrices has involved complex concentrations too low for useful optical limiting applications. Preliminary spectroscopic data obtained with these samples indicates that the lifetime and transient spectral behavior of the photoexcited complex does not change significantly from that of the complex in solution.

We are also beginning to explore use of other preformed polymers that may be dissolved with complexes and deposited on surfaces via spin coating or slow evaporation methods. For thin (< 1μm) films, concentrated solutions of polystyrene in chloroform can be deposited via dip coating. The limitation of this approach is that only relatively low concentrations of the transition metal complex salts can be prepared in solvents that dissolve polystyrene at high concentrations.

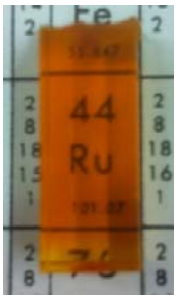

Figure D.1

More recently, using a suggestion of the Castellano group (Bowling Green State University, Ohio), we have begun preparing urethane elastomers containing chromophores. Figure D.1 shows a 1x1x2 cm block of $[(bpy)_2Ru(pyrvbpy)](PF_6)_2$ incorporated into a readily available commercial urethane, ClearFlex50®. Preparation of monoliths of the material containing various complexes is simple and relatively quick (hardening time of approx. 3 hr.). In addition, this particular material has a relatively low viscosity and allows the possibility of exploration of bimolecular reactions of encapsulated chromophores with added substrates. As can be seen, the materials have reasonably good optical quality and we have begun transient spectroscopic measurements using these monoliths.

E. 2DIR investigations of energy dissipation channels in chromophores

Efficient energy dissipation in optical limiters is essential for their durability, but the requirements for designing efficient energy relaxation pathways are currently not well understood. Electronic relaxation of optical limiting compounds results in their significant heating, which, depending on the size of the compound, can reach effective local excess temperatures of a thousand degrees centigrade. One of the goals of this project is to understand the principle of efficient energy dissipation on a molecular scale and to implement these principles in optical limiters. The process of energy dissipation is complex and involves different mechanisms.

A highly nonequilibrium vibrationally excited state is prepared as a result of full or partial electronic relaxation. Vibrational energy redistribution (IVR) is the most important process at small delay times after the relaxation. The excess energy, however, does not leave the molecule via IVR. Nevertheless, if the compound is large the IVR process includes a spatial

component; the energy redistribution into spatially remote modes would reduce the amount of excess energy in the vicinity of the metal center (for transition metal complexes). Thus, if the compound is designed correctly, the intramolecular IVR process can result in cooling of the most chemically active site in the molecule. Energy dissipation into the solvent (matrix) is another competing process, which eventually removes the excess energy from the compound. To design durable optical limiters it is important to understand both these processes.

The two-dimensional infrared spectroscopy (2DIR) method permits understanding the energy dissipation channels on a molecular level. In addition to measuring the energy dissipation rates dual-frequency 2DIR and relaxation-assisted 2DIR (RA 2DIR), the latter developed in Rubtsov laboratory, permit measuring the amount of energy transferred to a particular part of the molecular system (given that a vibrational reporter existed or has been placed in the targeted part of the molecular system). We used RA 2DIR spectroscopy to follow both components of the energy dissipation process – intramolecular energy redistribution (IVR) and dissipation to the solvent. A typical experimental design is shown in Fig. E1. The studied molecular systems contain an energy absorbing site (labeled as a star) and vibrational labels at the reporting site labeled with R_1, R_2, R_3. Excitation of the energy absorbing site causes a change of the reporter central frequency, which can be measured experimentally via 2DIR. Relaxation of the initially excited state (mode) causes energy dissipation. The reporter acts as a local thermometer – its central frequency changes when the excess energy arrives to the reporter site (RA 2DIR). Thus RA 2DIR is capable of following both the through bond IVR thermalization process as well as the dissipation process to the solvent and via solvent (matrix), depending on the location of the vibrational reporter in the molecular system.

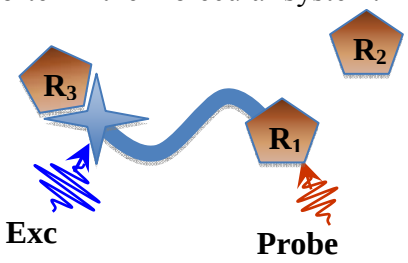

Fig. E1. Schematics of a molecular system for studying energy transport and energy dissipation dynamics. Excitation site (star) and three reporting sites (pentagons) are shown.

E.1. Energy dissipation to the solvent measured with the RA 2DIR technique

We have studied energy dissipation to the solvent in several molecular systems. Notice that increased sensitivity of the experimental setup permitted us observing, for the first time, very small temperature elevations (<0.1^{o}C). First experiments were performed on mixtures of two compounds where one contained the excitation site and the other contained the reporting site. Fig. E2A shows how the thermalization occurs for the case of (mutually) randomly distributed molecules N,N-dimethyl nicotinamide and 4-azido-butan-2-one in chloroform. Here the N≡N / amide-I cross-peak amplitude reports on the temperature increase at the amide as a function of time delay following excitation of the azido moiety. The thermalization occurs with a characteristic time of 18.7 ps and is essentially complete by 50-60 ps at concentrations of both reagents of 80 mM.

The result is different if the vibrational label pairs (excited and reporting) are not randomly distributed, but instead tethered to each other. Fig. E2B shows the energy transport dynamics in the host-guest complex of azidopermethylated cyclodextrin (host) and ademantylamide (guest). A clear induction period indicates that the IR labels cannot come to a

close contact to each other; indeed a minimal distance of ca. 9Å is expected for this complex from the DFT modeling. The rise time, that follows the induction period, is much faster than that for the random mixture.

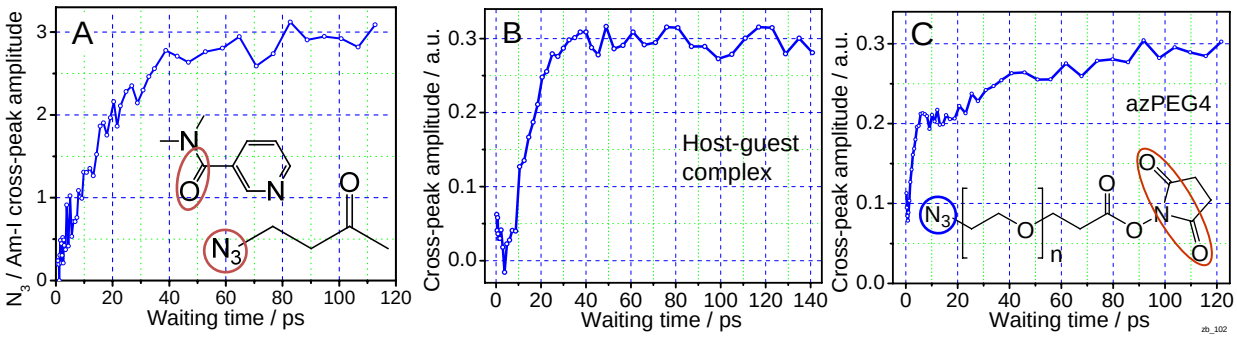

Fig. E2. Waiting-time N_3/amide-I or N_3/C=O cross-peak dependencies (A) for a 1:1 mixture of compounds shown in the inset, (B) for a 1:1 host-guest complex (see text), and (C) for azPEG4, all in chloroform.

In the third system the initially excited and reporting IR labels belong to the same molecule and are, therefore, connected by a covalent backbone. Two energy dissipation regimes can be observed simultaneously (Fig. E2C, azPEG4). The plateau indicates a thermal contribution associated with the energy transport via the solvent; a less pronounced peak at ca. 8 ps is due to energy transport via covalent backbone. Notice that the dissipation via solvent dominates here only because the experiment is done in a pure azPEG4 liquid (very high concentration). A mean end-to-end distance in PEG4 oligomer assuming a random coil structure in chloroform (Mark-Houwink exponent of ~0.68) was calculated to be ca. 9Å. No induction period is found due to a wide distribution of end-to-end distances, partially caused by its high concentration. The data (Fig. E2) are not published yet, but the manuscript is under reparation.

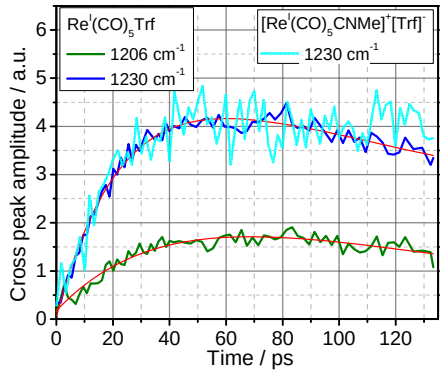

Fig. E3. Waiting-time dependence for the cross-peaks between carbonyl asymmetric stretching mode (~2058 cm^{-1}) and SO and C-F (1230 and 1206 cm^{-1}) stretching modes for $Re(CO)_5Trf$ and $[Re(CO)_5(CNMe)]^+[Trf]^-$ compounds in chloroform.

Energy transport to the counterion from transition metal complex was investigated in a rhenium(I) pentacarbonyl(acetonitrile) complex with triflate counterion and compared to that in the pentacarbonyltriflate complex (Fig. E3). The cross peaks between CO stretching (2058 cm^{-1}) and SO and C-F (1230 and 1206 cm^{-1}) stretching modes were recorded as a function of the waiting time. The similarity of the kinetics obtained for two complexes (blue and cyan lines in Fig. E3) and the slow scale of the relaxation indicate that the CO relaxation occurs to the solvent and does not involve the pathway to the acetonitrile ligand to any extent. These experiments emphasize the necessity of assessing experimentally the relaxation dynamics and pathways in transition metal complexes as coordination bonds can either offer relaxation pathways as in ref. [Kasyanenko, et al. *J. Chem. Phys.*, 2009, **131**, 154508] or serve as a break of relaxation pathways (as in Fig. E3).

E.2. Intramolecular energy redistribution: Energy transport via a polymer chain

Over the last several years we have investigated energy dissipation in various molecular systems, including model compounds, polymers, and transition metal complexes (see references in

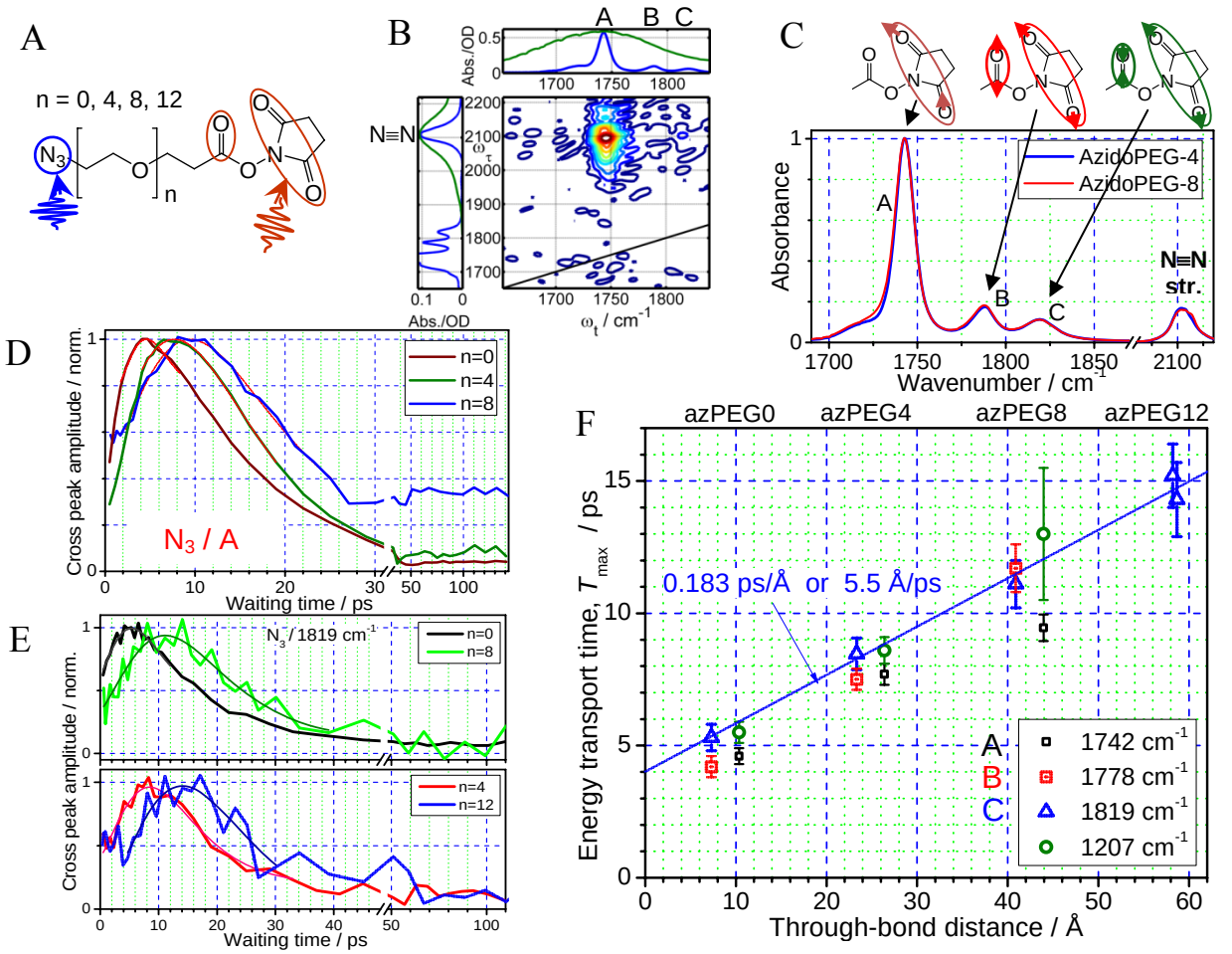

Fig. E4. Set of graphs illustrating ballistic energy transport in PEG oligomer chains. (A) Structures of the studied compounds featuring an azido moiety (excited by a fs laser pulse), PEG bridge of variable length, and succinimide ester featuring three carbonyl transitions (C) serving for probing the excess energy (temperature) as a function of time delay between excitation and probing. (B) an example of dual-frequency 2DIR spectrum, showing cross peaks between N≡N stretching mode of the azido moiety and carbonyl stretching modes of succinimide ester. (C) Linear absorption spectra of azPEG4 and azPEG8 in chloroform and peak assignment (DFT based). Cross-peak amplitude as function of the waiting time (D) for azPEG0, 4, and 8 (N≡N / peak A) and (E) for azPEG0, 4, 8, and 12 (N≡N / peak C). (F) Energy transport time, T_{max}, as a function of through-bond distance. The distances were calculated from the central nitrogen atom of the azido moiety to the carbon atom of the ester for modes at 1778 and 1819 cm^{-1} and to the nitrogen atom of succinimide for modes at 1742 and 1207 cm^{-1}.

[Rubtsov, Acc. Chem. Res., 2009, **42**, 1385-1394] and ref. Kasyanenko, et al. *J. Chem. Phys.*, 2009, **131**, 154508; Keating et al. *J. Phys. Chem. C*, 2010, **114**, 16740). To summarize the previous results pertinent for this project, we found that (i) cooling in transition metal complexes having small ligands, such as dithiolate, bipyridine and some others, occurs on a 20 ps time scale; (ii) the vibrational energy propagates efficiently via coordination bonds; (iii) the energy transport time correlates with the through-bond distance; and (iv) the energy transport mechanism in several compounds is diffusive with a rate of ca. 2 Å/ps.

During the last year we have investigated how the rates of energy transport and energy dissipation depend on the length of the polymer chain. A series of PEG oligomers featuring 0, 4, 8, and 12 repeating PEG units caped with an azido moiety (excitation) on one end and succinimide ester reporter on another end were investigated (Fig. E4A). We discovered that the energy transport via the oligomer chain is very efficient. The reason for the high efficiency of the transport is in formation of an optical phonon, which propagates through-bond in the chain with a constant speed of 550 m/s (5.5 Å/ps). This mechanism, which has not been previously demonstrated for molecules in solution, permits delivering energy from the place it has been absorbed at as a photon to 60 Å distance and it takes only ca. 15 ps. Application of vibrational signaling in molecular electronics can be envisioned. It is conceivable that it could be used for efficient cooling of optical limiters. The results have been recently published in PNAS and PCCP journals.

Figure E4 presents a set of graphs describing the experiments performed in this work. Fig. E4B shows an example of dual-frequency 2DIR spectrum, focusing at the cross peaks between N≡N stretching mode of the azido moiety and carbonyl stretching modes of succinimide ester (labeled as modes A, B, and C); Fig. E4C shows the mode assignment. Figures E4D&E show how the cross-peak amplitude depends on the waiting time – the dynamics that is associated with energy arrival from N_3- to the succinimide ester moiety.

The energy transport time, T_{max}, as a function of through-bond distance is plotted in Fig. E4F for four different cross peaks (indicated on the graph). A linear relation found between the T_{max} and the distance indicates a ballistic energy transport via covalent bonds.

Thus we found that covalent bonds provide an efficient network for dissipation of vibrational energy, including a ballistic transfer (Fig. E5). A compound with high optical limiting properties may need to be decorated with (multiple) aliphatic chains to provide efficient energy dissipation channels.

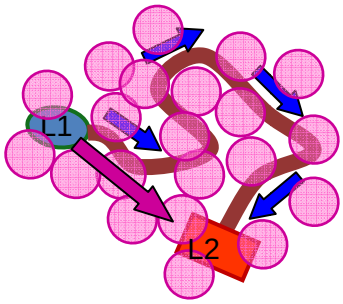

Fig. E5. Energy dissipation with through-bond (blue arrows) and through-solvent (red arrow) contributions.

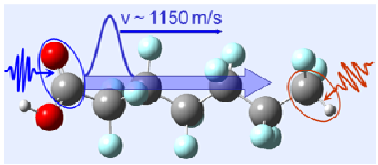

The coiled structure of PEG oligomers results in additional disorder of the chain states, which is expected to reduce the ballistic transport efficiency. Perfluoroalkane chains are known to form rod-like structures with antiperiplanar orientation of the neighboring carbon atoms both in solution and in crystals; such regularity may lead to even more efficient energy transport. We have investigated energy transport in a series of perfluoroalkane oligomers with various chain lengths of 3, 5, 7, 9, and 11 carbon atoms terminated by a carboxylic acid moiety on one end and $–CF_2H$ group on another end (Fig. E6A). Indeed the states of the bridge were found to be strongly delocalized (Fig. E6D); note that delocalization factor of eight is expected for the C9 compound in the case of full delocalization over eight oligomeric sites of C9. The energy transport initiated

by exciting the C=O stretching mode of the acid was recorded by measuring a cross-peak amplitude between the C=O stretch and the C-H bending mode (Fig. E6C) as a function of the waiting time between the excitation and probing (Fig. E6E,F). A linear dependence of energy transport time vs. chain length was found, which suggests a ballistic energy transport mechanism (Fig. E6G). The energy transport speed, measured from the chain-length dependence of the half-rise time, $T_{½}$, was found to be ca. 1150 m/s, which is close to the longitudinal speed of sound in Teflon polymers (1300 m/s), suggesting that the wavepacket involving low-frequency modes of the chain likely contributes to the energy transport in perfluoroalkanes. It is conceivable that wavepackets involving other bands, including the optical bands of the chain, also contribute to the energy transport in perfluoroalkane oligomers.

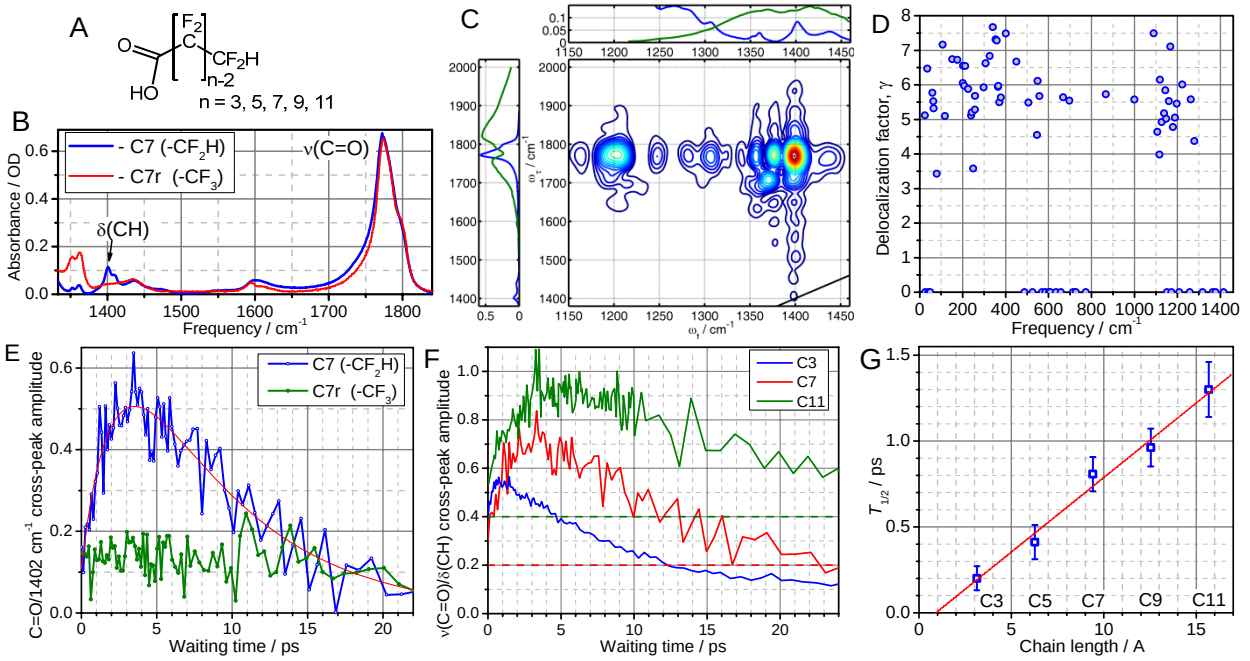

Fig. E6. (A) Structure of C*n* compounds. (B) Linear absorption spectra of the C7 and C7r (reference, terminated with CF3 moiety) compounds in $CDCl_3$. (C) 2DIR spectrum of the C5 compound measured at the waiting time of 3.0 ps. The linear absorption spectrum (blue lines) and the spectra of IR pulses (green lines), are shown in the attached panels. (D) Delocalization factor, γ, as a function of mode frequency for C9. (E) Waiting time dependences of the ν(C=O)/1401 cm^{-1} cross peak for the C7 and C7r compounds. (F) Waiting time dependences of the ν(C=O)/δ(CH) cross peak measured for the C3, C7, and C11 compounds. For clarity, constant values of 0.2 and 0.4 were added to the C7 and C11 data. (G) Dependence of T_{max} on the chain length.

E.3. Characterization of polarization extent in the excited electronic states in transition metal complexes using time resolved mid-IR spectroscopy.

Understanding the nature of excited electronic states in transition complexes is extremely important for predicting their optical limiting properties. Pump-probe spectroscopy in the visible spectral range is instrumental in addressing the question, although has limited sensitivity of the polarization extent of the excited states. Such polarization affects greatly the two-photon cross sections as well as excited state absorption properties. At Tulane we have implemented time-resolved mid-IR spectroscopy (TRIR) that features ca. 60 fs time resolution. Figure E7 illustrates how the extend of charge separation in the rhenium(I) complexes is changing in a set of compounds where the donor strength of one of the ligands is varied. As expected, an MLCT

(Re→bpy) excited state is formed in the RePhCN complex (Fig. E7) upon electronic excitation; the state features a long lifetime of several microseconds. Formation of the MLCT state is clearly seen from the spectral changes in the CO region (1900-2080 cm^{-1}), Fig. E7. In the

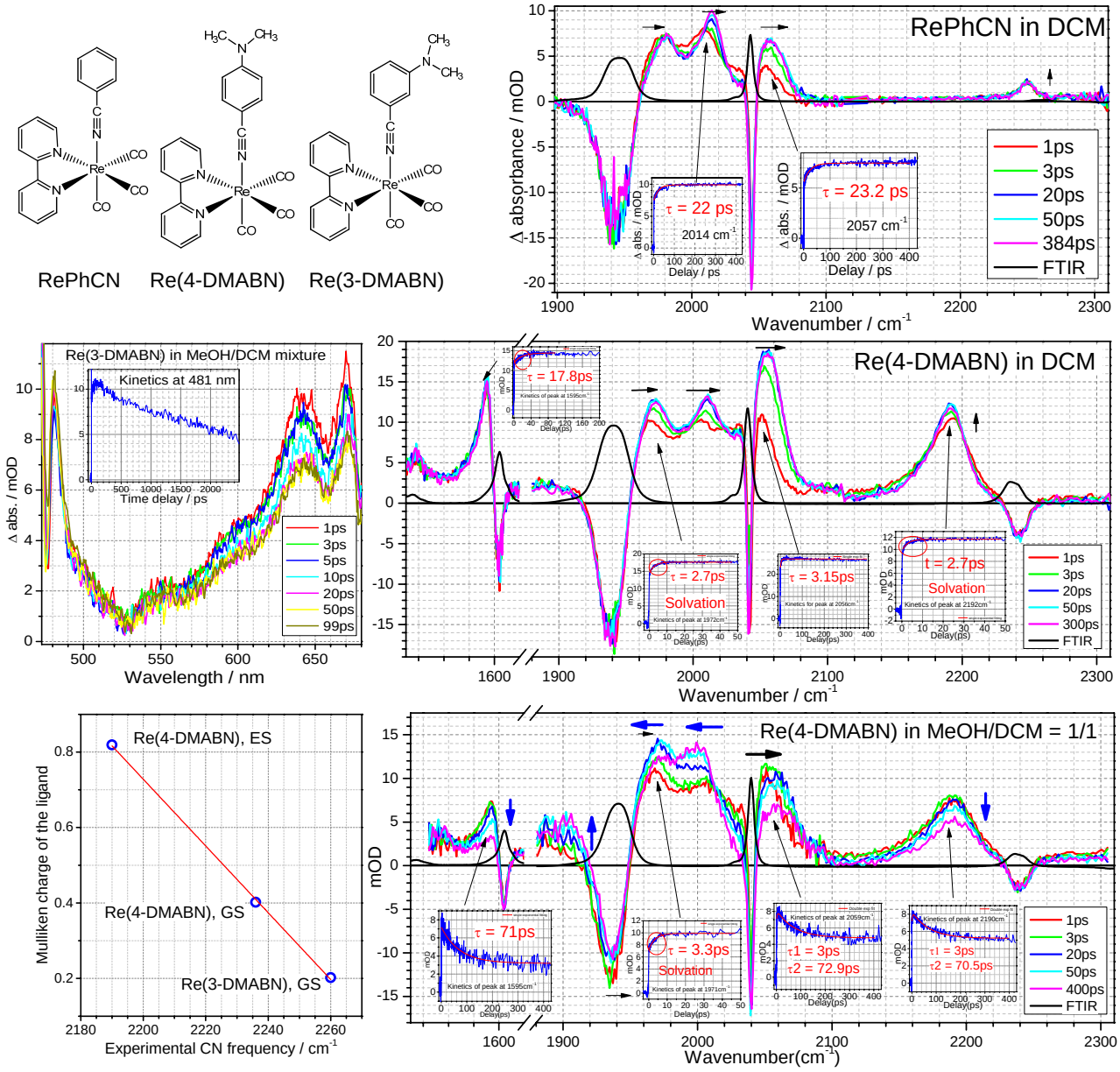

Fig. E7. TRIR spectroscopy of a set of Re(I) compounds featuring ligands with various donor strength. Left bottom graph shows a linear relation between the DFT computed Mulliken charge of the DMABN ligand and experimental frequencies of the C≡N stretching mode.

compounds featuring ligands with strong electron donor capabilities the visible transient absorption spectra were found to be similar. Based on the common wisdom one would predict formation of a similar MLCT state upon excitation, which could decay into a charge separated state (LLCT) with a cation radical at the DMABN ligand. Instead, as clearly shown by TRIR spectroscopy (Fig. E7, stretching frequencies at ca. 2240, C≡N, and 1600 cm^{-1}, C-C of the

phenyl ring), immediately upon excitation a mixed MLCT/LLCT state is formed in both DCM and in methanol/DCM mixture. Further evolution of the excited state in DCM is small and can be fully attributed to solvation dynamics. In the mixed solvent, however, the transient spectrum changes with a characteristic time of ca. 70 ps, which can be attributed to conformational changes of the DMABN ligand. Importantly, using the TRIR data, the extent of charge separation can be evaluated in each complex and in each state involved. This approach will allow us better predicting the optical limiting properties of transition metal complexes which will be / are synthesized in Schmehl laboratory at Tulane.

Table E1. DMABN ligand charge and CN stretching frequency in ground (GS) and excited (ES) states.

	RePhCN, GS	Re(3-DMABN) GS	Re(3-DMABN) ES	Re(4-DMABN) GS	Re(4-DMABN) ES
DMABN ligand charge	0.192	0.202	0.34	0.402	0.82
CN frequencies (cm^{-1})	2344	2360	2343	2316	2268
Re-N-C angle	179.8	178.6		179.4	175.4

F. Archival Publications:

"Constant-speed vibrational signaling along polyethyleneglycol chain up to 60Å distance", Z. Lin and I. V. Rubtsov , *Proc. Natl. Acad. Sci. U.S.A.*, 2011, **109**(5) 1413-1418. DOI: 10.1073/pnas.1116289109.

" Modified terpyridyl Ru(II) amine complexes with prolonged room temperature excited state lifetimes: role of intramolecular energy transfer", J. Gu, Y. Yan, B. J.Helbig and R. H. Schmehl, manuscript in preparation.

Z. Lin, N. Zhang, J. Jayawickramarajah, I. V. Rubtsov, Ballistic energy transport along PEG chains: Distance dependence of the transport efficiency; (invited) *Phys. Chem. Chem. Phys.* (2012) **30**(14), 10445-10454. DOI: 10.1039/c2cp40187h

N. I. Rubtsova, I. V. Rubtsov, Ballistic energy transport via perfluoroalkane linker. *Chem. Phys.,* accepted.

Z. Lin, N. I. Rubtsova, V. V. Kireev, I. V. Rubtsov, Ballistic energy transport in PEG oligomers, In *Springer Series in Chemical Physics*; M. Chergui, A. Taylor, Eds.; Springer, (2013), in press.

"Evaluation of charge transfer extent in excited states of rhenium(I) complexes using time-resolved vibrational spectroscopy"; Y. Yue, T. Grussenmyer, D. Beratan, I.V. Rubtsov, R. Schmehl; manuscript in preparation.